

RESEARCH

Open Access



# High-strength collagen/delphinidin film incorporated with *Vaccinium oxycoccus* pigment for active and intelligent food packaging

Simiao Yin<sup>1</sup>, Yuanzhi Zhang<sup>1</sup>, Xiaoxia Zhang<sup>1</sup>, Keyu Tao<sup>2</sup> and Guoying Li<sup>1\*</sup> 

## Abstract

This study developed an active and intelligent collagen-based packaging film with high strength for visually monitoring the freshness of fish. The results of scanning electron microscopy and atomic force microscopy showed that the film based on cross-linked collagen/delphinidin catalyzed by laccase exhibited a denser layer structure and a rougher surface. The dry and wet tensile strengths of the laccase-catalyzed collagen/delphinidin film (Col/Dp-LA film) increased by 41.74 MPa and 13.13 MPa in comparison with that of the pure collagen film, respectively. Moreover, the Col/Dp-LA film presented good antioxidant and barrier properties demonstrated by the results of free radical scavenging rate, light transmission rate, and water vapor permeability. The intelligent collagen-based film was obtained by incorporating *Vaccinium oxycoccus* pigment into the Col/Dp-LA film, which could change color under different pH values. When applied to the preservation of fish fillets, the film could release Dp to minimize oxidative rancidity and prolong the shelf life of the fish for 2 days. Meanwhile, the film showed visual color changes from purplish-red to greyish-blue after the fish spoilage. These results indicated that the collagen film treated with delphinidin, laccase, and *Vaccinium oxycoccus* pigment has potential application value in the field of active and intelligent food packaging.

**Keywords** Collagen, Delphinidin, Laccase, *Vaccinium oxycoccus* pigment, Food packaging film

\*Correspondence:

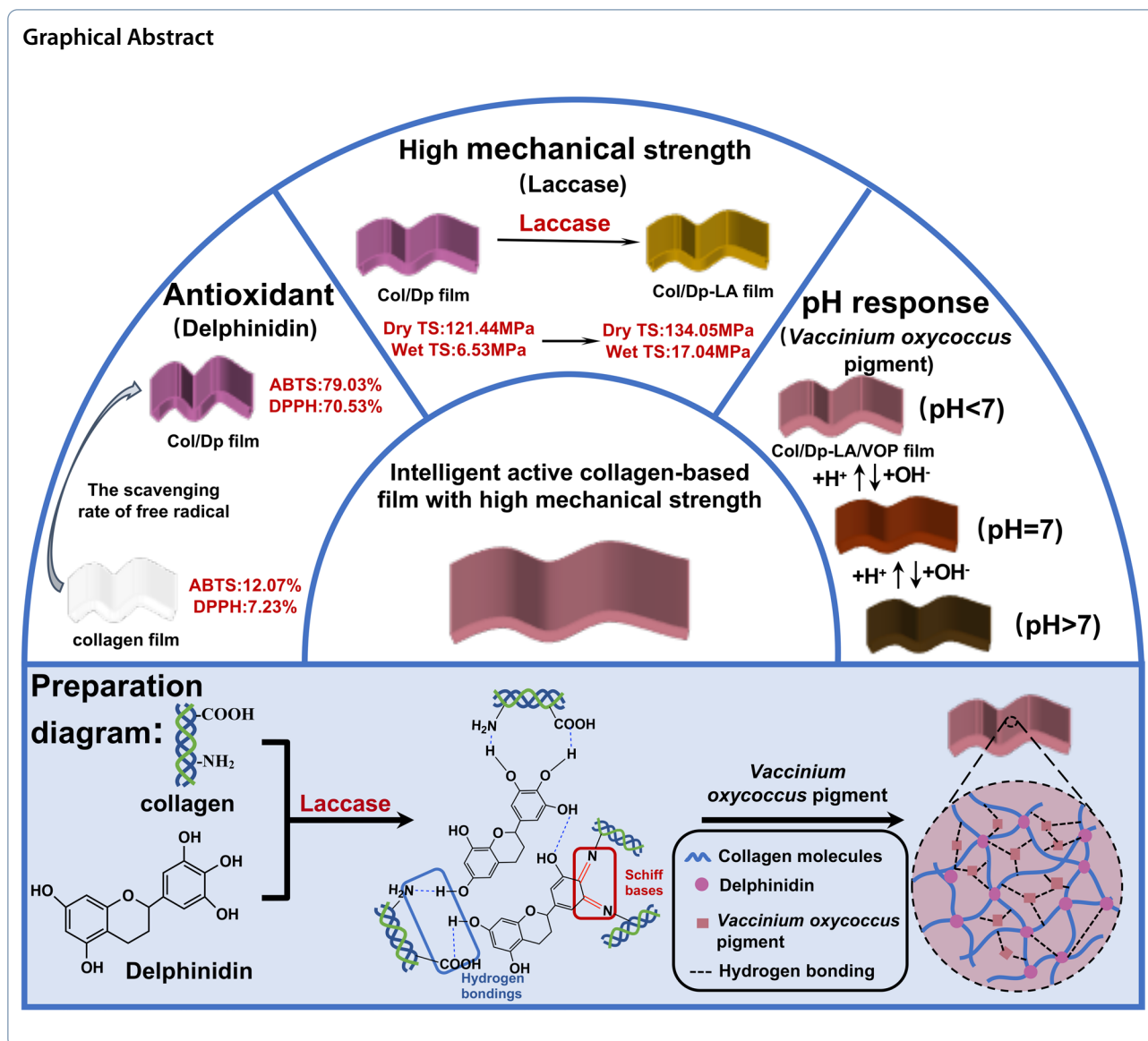
Guoying Li

liguoyings@163.com

Full list of author information is available at the end of the article



© The Author(s) 2023. **Open Access** This article is licensed under a Creative Commons Attribution 4.0 International License, which permits use, sharing, adaptation, distribution and reproduction in any medium or format, as long as you give appropriate credit to the original author(s) and the source, provide a link to the Creative Commons licence, and indicate if changes were made. The images or other third party material in this article are included in the article's Creative Commons licence, unless indicated otherwise in a credit line to the material. If material is not included in the article's Creative Commons licence and your intended use is not permitted by statutory regulation or exceeds the permitted use, you will need to obtain permission directly from the copyright holder. To view a copy of this licence, visit <http://creativecommons.org/licenses/by/4.0/>.

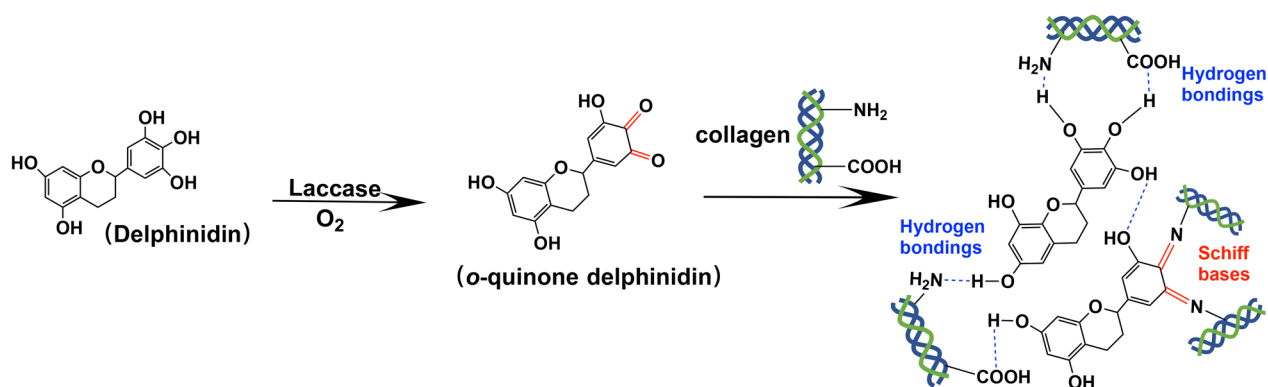


## 1 Introduction

In recent years, active edible packaging films composed of natural film-former and functional additives have significantly emerged for food packaging with safety, activity, and functionality [1]. Proteins, such as collagen [2], soy protein [3], and wheat gluten protein [4], are good film-former exhibiting security and barrier properties. Collagen has been successfully commercialized in the production of sausage casings exhibiting edibility, availability, good barrier property, and mechanical property [5]. The development of functional collagen packaging film has been considerable attention with the increase in requirements for additional protection and control of food products [6]. Antioxidants and pH-sensitive pigments are frequent ingredients to be

introduced into the collagen matrix to improve functionality [7].

Antioxidants incorporated into food packaging film can prevent food oxidation so as to prolong the shelf life of products [8]. Natural antioxidants are ideal active additives to endow antioxidant activity to collagen film because natural antioxidants have greater safety compared to synthetic antioxidants [9, 10]. Polyphenols are natural plant-derived antioxidants with multiple phenolic groups which can quench free radicals to control the lipid oxidation of products [11]. Moreover, the phenolic groups of polyphenols can form multipoint hydrogen bonds with amino acid residuals in collagen side chains, and the hydrogen bonds are beneficial to improve the mechanical strength of collagen film [12, 13]. Lots of



**Scheme 1:** Schematic diagram of laccase-catalyzed delphinidin and the interaction between collagen and laccase-catalyzed delphinidin

studies have shown that the introduction of polyphenol oxidases into the collagen/polyphenol systems can further enhance the binding stability between collagen and polyphenols [14–16]. Laccase, as a multi-copper polyphenol oxidase, is considered bio-friendly because it performs the catalysis process using molecular oxygen as the only co-substrate and yields water as the sole by-product [17, 18]. Laccase selectively oxidizes primary o-phenols to reactive o-quinone which can form covalent Schiff bases with the amino of collagen side-chains [19, 20]. As mentioned in Jus's study, the use of laccase in collagen/phenolic compound systems could enhance the crosslinking between collagen and phenolic compounds, which brought better tensile strength than the collagen sample upon treatment with polyphenol alone [21]. In a similar result described by Tian et al., the tensile strength of the collagen film treated with laccase-catalyzed galotannins increased by 11.15 MPa in comparison to the ones modified with galotannins alone [22]. The cross-linked collagen/polyphenol systems catalyzed by laccase improve the collagen-based film with antioxidant activity and further ameliorate their mechanical property.

pH-sensitive pigments endow the film with pH responsive to intelligently monitor the food quality in real-time by color responses, that is, a visual color change corresponding to the change in pH value due to volatile amines released from food (e.g. meat, fish) putrefaction [23, 24]. Natural and food-grade dyes are attractive options because it is easy to meet the expectations about food safety of current consumers [25]. As healthy and edible colorimetric indicators, anthocyanins extracted from plants have been evidenced they could present different colors with altering acidic/alkaline conditions, and their sensing property is efficient in food packaging [26, 27]. Shi et al. used blueberry anthocyanins to prepare a pH-sensitive film for monitoring the freshness of *Tilapia*, and the color of the film altered from purple

to blue-purple with the increase in pH value caused by *Tilapia* fillets deterioration [28]. Ran et al. successfully developed a film with a continuous color response by loading grape-skin red on the soy protein film to indicate the situation of pork spoilage and found that the hydrogen bonds and electrostatic interactions were between Grape-skin red (GSR) and soy protein [29]. Anthocyanins with good pH sensitivity and reactive activity are suitable for developing intelligent collagen-based packaging film to provide visualized information for the product quality status inside the package [30].

In this study, we developed active and intelligent packaging film by using two substances of collagen and delphinidin (Dp) as the film-forming matrix, laccase (LA) as the crosslinker of the film matrix, and *Vaccinium oxycoccus* pigment (VOP) as the pH-sensing indicator. The materials chosen in the study are non-toxic, reproducible, and biodegradable that can eliminate public concerns about food safety and environmental issues. Dp with o-triphenolic structure could be specifically catalyzed by LA to synergistically enhance the mechanical strength and antioxidant activity of the collagen film (Scheme 1). In addition, the effects of modifying the collagen film with LA and Dp on the structure, thermal stability, water-resisting property, and light barrier property of the film were evaluated. The intelligent pH sensitivity was obtained by using VOP. The film was applied to the preservation of the fish fillets stored at  $4\text{ }^{\circ}\text{C} \pm 1\text{ }^{\circ}\text{C}$  for 10 days (d) to evaluate its application potential in active and intelligent food packaging.

## 2 Materials and methods

### 2.1 Raw materials

Lyophilized bovine skin collagen was obtained according to the method of Yang et al. [31]. The treated bovine skin was minced and placed in 0.5 M acetic acid containing 3% pepsin to extract at  $4\text{ }^{\circ}\text{C}$  for 3 d. The extract was

centrifuged to obtain the supernatant. 0.7 M sodium chloride was added to the supernatant to salt out collagen and the precipitate was taken by centrifugation. The precipitate was dissolved with 0.5 M acetic acid and then dialyzed, and the dialyzed collagen solution was lyophilized at  $-60\text{ }^{\circ}\text{C}$  in a freeze dryer and set aside for later use. LA, with the enzymatic activity of 120 u/g from *Trametes Versicolor*, was obtained from Yuanye Biotechnology Company. Dp was purchased from Xian Lanzhide Biotechnology Co. (industrial grade). VOP was supplied by Shandong Shengjiade Biotechnology Co. (industrial grade). All of the other reagents were analytical grade and purchased from Shanghai Aladdin Bio-Chem Technology Co., Ltd.

## 2.2 Preparation film of collagen and delphinidin

The lyophilized collagen was dissolved in 0.1 mol/L acetic acid at  $4\text{ }^{\circ}\text{C}$  for 12 h to obtain a homogeneous collagen solution with a concentration of 6 mg/ml. Delphinidin powder was also dissolved in 0.1 mol/L acetic acid to reach a concentration of 0.6 mg/ml. Mix the two solutions at 5: 1 under vigorous magnetic stirring for 4 h (h) at  $4\text{ }^{\circ}\text{C}$  to obtain a collagen/delphinidin mixed solution. Subsequently, 10% of glycerin (w/w, delphinidin/collagen dry weight) was added into the mixed solution as a plasticizer. After the solution was mixed well, the solution was degassed by refrigerated centrifugation for 10 min (min), and then cast into the self-designed silicon mold ( $10\text{ cm} \times 10\text{ cm}$ ). The mixed solution was dried at  $25\text{ }^{\circ}\text{C} \pm 1\text{ }^{\circ}\text{C}$  for 4 d. The dried films were placed in the controlled environment chamber ( $50\% \pm 2\%$  relative humidity and  $25\text{ }^{\circ}\text{C} \pm 1\text{ }^{\circ}\text{C}$ ) for 3 d before use. Pure collagen film was recorded as “Col film”. The collagen/delphinidin mixed film was recorded as “Col/Dp film”.

A LA solution with the enzymatic activity of 1 u/ml was prepared by dissolving 0.5 g of LA (120 u/g) in 60 ml deionized water. The Col/Dp film was immersed in the LA solution for 4 h at  $25\text{ }^{\circ}\text{C} \pm 1\text{ }^{\circ}\text{C}$ . After 4 h, the film was rinsed three times with distilled water to wash away the LA from the surface of the film. The film was dried at  $25\text{ }^{\circ}\text{C}$  for 24 h and balanced in the controlled environment chamber ( $50\% \pm 2\%$  relative humidity and  $25\text{ }^{\circ}\text{C} \pm 1\text{ }^{\circ}\text{C}$ ) for 3 d before use. The prepared film was recorded as “Col/Dp-LA film”.

## 2.3 Microstructural analysis

### 2.3.1 Scanning electron microscopy (SEM)

The cross-sectional microstructures of the films were observed by Scanning electron microscopy (Apreo 2C, Thermo Fisher, Massachusetts, USA) with an accelerating voltage of 15 kV.

### 2.3.2 Atomic force microscope (AFM)

The surface roughness of the films was determined by a SHIMADZU SPM-9600 Atomic Force Microscope (SHIMADZU, Japan) instrument by the MFP-3D AFM operating in tapping mode under ambient air conditions.

## 2.4 Properties testing

### 2.4.1 Differential scanning calorimetry (DSC)

The thermostabilities of the films were evaluated by DSC-204F01 (NETZSCH Co, Germany) in the temperature range  $20\text{--}100\text{ }^{\circ}\text{C}$  at a heating rate of  $10\text{ }^{\circ}\text{C}/\text{min}$  and a nitrogen flow rate of 40 mL/min.

### 2.4.2 Thickness

The thickness of the films were measured according to the Chen et al. with a minor modified [32]. To accurately measure the thickness of the films, five sites of each film were randomly selected, and the cross-section thickness of the films was specially measured by using electronic digital micrometer (model 211-101F, Guangxi, China).

### 2.4.3 Mechanical property

Each film sample was cut into  $45\text{ mm} \times 5\text{ mm}$  strips to test the dry tensile strength, wet tensile strength, dry elongation at break, and wet elongation at break by a universal testing machine (UTM2102, New Sansi, Shenzhen, China). The dry strength and elongation at break were tested by stretching mode in the vertical direction at a constant speed of 10 mm/min. The wet strength and elongation at break measurements were used in the same mode after pre-immersing the films in distilled water for 2 min.

The tensile strength was calculated using the Eq. (1):

$$\text{Tensile strength (MPa)} = \frac{F}{d \times W} \quad (1)$$

where F is the maximum tension when the film breaks (N), d is the thinness of the film (mm), W is the wideness of the film (mm).

The Elongation at break was calculated using the Eq. (2):

$$\text{Elongation at break (\%)} = \frac{L - L_0}{L_0} \times 100\% \quad (2)$$

where L is the line distance when the film breaks (mm),  $L_0$  is the line distance of the original film (mm).

### 2.4.4 Water vapor permeability (WVP)

WVP values of the three samples were measured according to the method of Liu et al. [33]. A 75% relative humidity circumstance was established in the desiccator with

saturated sodium chloride (NaCl) aqueous solution. Each film sample was covered on the top of the beaker that contained anhydrous calcium chloride (0% relative humidity) and then placed in the test chamber at 25 °C and 75% relative humidity. The WVP value was measured by weighing beakers at an interval of 2 h within 5 d and WVP ( $\text{g}\cdot\text{mm}^{-2}\cdot\text{s}^{-1}\cdot\text{Pa}^{-1}$ ) was calculated by Eq. (3).

$$\text{WVP} = \frac{W \times d}{\Delta t \times A \times \Delta P} \quad (3)$$

In this equation,  $W/\Delta t$  is the weight gain over time ( $\text{g}\cdot\text{s}^{-1}$ ),  $d$  is the average thickness of the film (mm),  $A$  is the bottle top area ( $\text{mm}^2$ ) and  $\Delta P$  (Pa) is the vapor pressure difference across the film.

#### 2.4.5 Water solubility

The water solubilities of the films were experienced using the method of Choo et al. with minor modifications [34]. Each film sample was cut into 2 cm × 2 cm pieces. The pieces were dried at 105 °C for 4 h and were then weighted to obtain the initial weight ( $W_0$ ). The dried films were then placed in distilled water at 25 °C for 24 h and filtered through Whatman No. 1 filter paper. The residue collected on the filter paper was again dried at 105 °C for 24 h and was then weight (recorded as  $W_1$ ). Water solubility (%) was calculated by Eq. (4)

$$\text{Water solubility (\%)} = \frac{W_1 - W_0}{W_0} \times 100\% \quad (4)$$

#### 2.4.6 Optical property

The optical properties of the films were evaluated by measuring the transmittance of the films in the range of 200–800 nm on a UV-vis spectrophotometer (UV-2600, Shimadzu, Japan). The light transmittance of the films was then calculated by the following Eq. (5) based on their OD.

$$\text{Light transmittance (\%)} = \frac{1}{10^{\text{OD}}} \times 100\% \quad (5)$$

where OD is the absorbance of the films at different wavelengths.

#### 2.4.7 Antioxidant activity

The antioxidant properties of the films were evaluated using DPPH and ABTS scavenging activity according to the method of Tang et al. with minor modification [35]. Briefly, each film (4 mg) was immersed in 4 mL ABTS and DPPH free radical working solutions for 30 min in the dark, respectively. After the reaction, the ABTS scavenging rate was obtained by the equation as follows:

$$\text{ABTS scavenging activity (\%)} = \left[ \frac{A_0 - A_s}{A_0} \right] \times 100\% \quad (6)$$

where  $A_0$  is the absorbance of the ABTS radicals working solution at 734 nm, and  $A_s$  is the absorbance of the ABTS radicals working solution at 734 nm after treatment with the film.

The DPPH scavenging activity was calculated by the following equation:

$$\text{DPPH scavenging activity (\%)} = \left[ \frac{A_1 - A_2}{A_1} \right] \times 100\% \quad (7)$$

where  $A_1$  is the absorbance of the DPPH radicals working solution at 517 nm, and  $A_2$  is the absorbance of the DPPH radicals working solution at 517 nm after treatment with the film.

### 2.5 Development of pH-sensitive packaging film

The Col/Dp-LA film was immersed in a 5 mg/ml VOP solution for 4 h at 25 °C. After 4 h, the film was rinsed three times with distilled water to wash away VOP from the surface of the film. Then, the film was placed in a desiccator with a relative humidity of  $50\% \pm 2\%$  at  $25 \text{ °C} \pm 1 \text{ °C}$  for at least 2 days. The prepared film was named “Col/Dp-LA/VOP film”.

#### 2.5.1 UV-Vis spectroscopy of VOP solutions and color variation of the Col/Dp-LA/VOP film

The UV-Vis spectra of VOP solutions was measured by a UV-Vis spectrophotometer (UV-2600, Shimadzu, Japan) in the range of 400–800 nm. The pH value of VOP solution was adjusted by adding 1 mol/L NaOH or HCl. Each of the four Col/Dp-LA/VOP films (1 cm × 2 cm) was immersed in 5 ml buffer with different pH values (5.0–9.0).

#### 2.5.2 Application of the Col/Dp-LA/VOP film for monitoring the freshness of the fish fillets

Largefin longbarbel catfish (*Ictalurus punctatus*) purchased from a supermarket, and then was skinned and sliced.  $20 \text{ g} \pm 0.5 \text{ g}$  fish fillets were packaged inside the Col film and the Col/Dp-LA/VOP film, respectively. The packaged fish fillets were then stored in plastic dishes at a relative humidity of  $75\% \pm 1\%$  and a temperature of  $4 \text{ °C} \pm 1 \text{ °C}$  for 10 d. The 2-thiobarbituric acid reactive substances (TBARs), total volatile basic nitrogen (TVB-N), and pH values of the fish fillets were then tested every 2 days until the end of storage time.

**2.5.2.1 Determination of TBARs** 10.0 g fish fillets were added to 50 ml 7.5% (w/v) trichloroacetic acid (containing 0.1% EDTA) and then homogenized at 15,000 rpm

till a uniform slurry was obtained. The dispersion was filtered through the filter fabric. 5 ml filtrate was added to 5 ml 0.02 mol/L 2-thiobarbituric acid reagent to boil for 30 min, and then the mixture was centrifuged at 2000 rpm for 10 min. Afterward, 5 ml supernatant was mixed with 5 ml chloroform, and then the mixture was stood until stratification. The absorbance of the upper liquid was measured at 532 nm and 600 nm. The formula was calculated as follows:

$$\text{TBARs value (mg/100 g)} = \frac{(A_{532 \text{ nm}} - A_{600 \text{ nm}})}{155} \times 726 \quad (8)$$

where  $A_{532 \text{ nm}}$  is the characteristic absorption peak of 3,5,5-trimethyl oxazole 2,4-dione formed by the reaction of thiobarbituric acid (TBA) with malondialdehyde.  $A_{600 \text{ nm}}$  is the non-specific absorptions of 3,5,5-trimethyl oxazole 2,4-dione, such as an increase in absorbance values caused by turbidity or color changes of the sample itself.

**2.5.2.2 Determination of TVB-N** The TVB-N values of the fish fillets packaged in the Col film and the Col/Dp-LA/VOP film were determined according to Cao et al. using a semi-micro Kjeldahl distillation unit every 2 days [36]. 100 ml distilled water was added to 10.0 g fillets and homogenized. The homogenate was distilled after adding 2.0 g MgO and the distillate was collected in a flask containing a 3% (w/v) aqueous solution of boric acid. Then, two drops of mixed indicator of methyl red and leaf methyl blue were added to the flask, and at this time the boric acid solution turned green. This was because the TVB-N produced by the distillation made the boric acid solution alkaline. Finally, the solution was titrated with 0.1 mol/L HCl solution until it turned pink. TVB-N value was expressed as mg of nitrogen per 100 g fillets (mg/100 g).

**2.5.2.3 pH measurements** The pH value of the fish fillets was measured according to AOAC (1995) [37]. 5.0 g fillets were homogenized in 50 ml distilled water to obtain a suspension. The suspension was filtered, and the pH of the filtrate was measured by using a pH meter (Rex PHS-3C, Shanghai INESA Scientific Instrument CO., LTD.). The pH of the filtrate was used to represent the pH of the fish fillet.

## 2.6 Statistical analysis

Each film was measured three times in parallel. The data of the experiments were expressed as the average  $\pm$  standard deviation (SD). The data were analyzed by using GraphPad Prism (GraphPad Software, San Diego,

California, USA). Duncan's multiple-range test was used to analyze the significance of differences between samples, and  $P < 0.05$  was set as a significance to compare the differences among the data.

## 3 Results and discussion

### 3.1 Microstructural analysis

The cross-section and surface morphology images of the Col film, Col/Dp film, and Col/Dp-LA film were observed by SEM and AFM, which are shown in Fig. 1. The Col film displayed a discontinuous cross-section, while the Col/Dp film and the Col/Dp-LA film showed more continuous, smooth, and homogeneous cross-sections. According to the areas marked by the red wireframes in Fig. 1a, the cross-section of the Col/Dp-LA film was the most compact of the three samples. A similar result was found by Qiang et al., that is, the collagen film showed a denser cross-section after being cross-linked with catalyzed catechins [38]. A possible explanation might be that LA-catalyzed Dp (Dp-LA) generated reactive o-quinones to form multipoint C=N covalent bonds with the amino groups of collagen [39]. In addition, FT-IR and XPS spectra were tested to further demonstrated the formation of covalent Schiff bases. The results showed that the characteristic peak attributed to C=O bonds was found in the FT-IR spectra of the Col/Dp-LA film, and the XPS spectra found that the content of C-N bonds in the Col/Dp-LA film (20.26%) was much higher than that in the Col film (13.00%). The relative experimental discussion was added to the Additional file 1: Fig. S1, S2.

The arithmetic roughness average of the surface ( $R_a$ ) and root mean square average of height deviations ( $R_q$ ) for each film was measured from the AFM images. The  $R_a$  value of the Col film was 1.29 nm, whereas the  $R_a$  value of the Col/Dp film was 0.97 nm and the  $R_a$  value of the Col/Dp-LA film was 1.56 nm. The value of  $R_q$  for the collagen film decreased from 1.25 to 1.18 nm with the addition of Dp, while the  $R_q$  value for the film rebounded to 2.06 nm with further catalysis by LA. It has been proven that the use of Dp and LA could change the surface property of collagen film [40, 41]. Katarzyna Adamiak et al. found that the  $R_a$  value of the film decreased from 114.93 to 112.28 nm after adding xanthohumol to the collagen matrix. The surface roughness of the film was reduced after the addition of Dp. This may be due to the good hydrogen bonding interaction between the phenolic hydroxyl group of Dp and the carboxyl group of collagen, and this interaction resulted in a uniform distribution of Dp in the collagen matrix. The use of LA increased the surface roughness of the film. This was because the stronger covalent interaction between Dp-LA and collagen further enhanced the cross-linking strength between

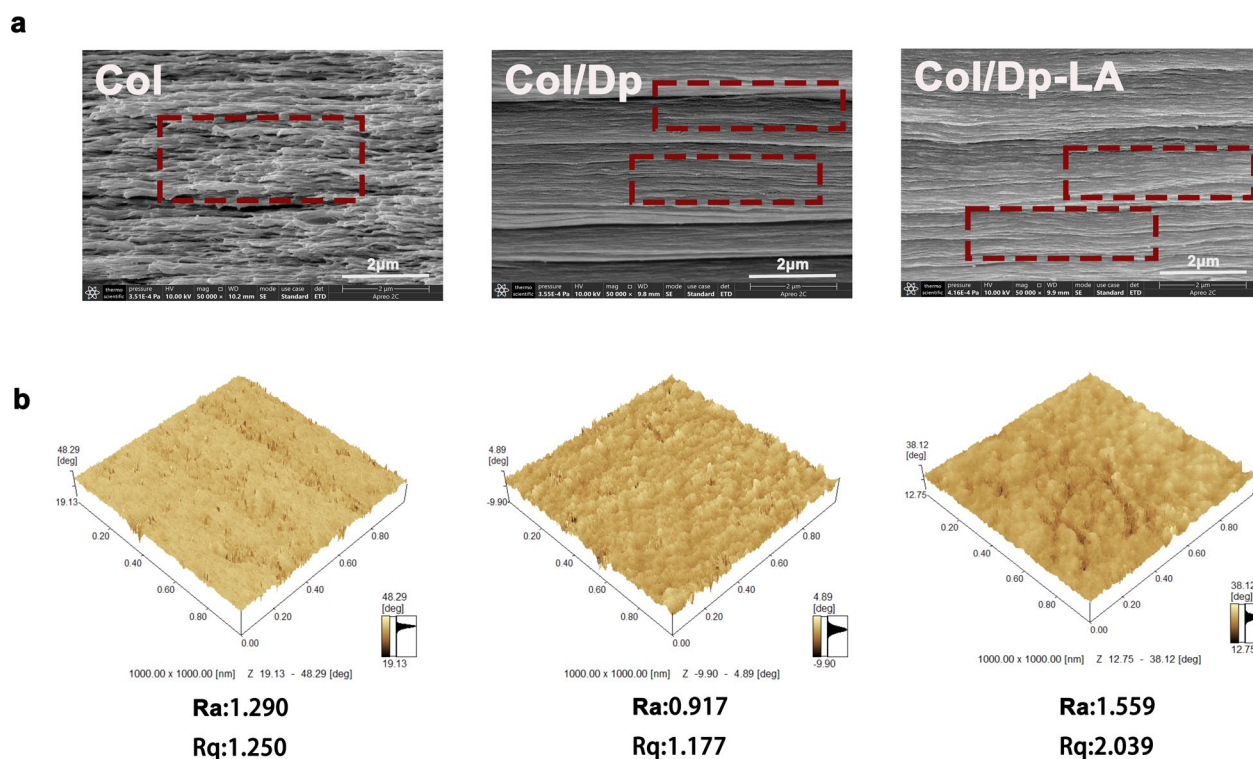


**Fig. 1** SEM cross-section images (scale bar is 2  $\mu\text{m}$  and the magnification is 50,000  $\times$ ) (The marked areas surrounded by red wireframes presented the compactness among the films) (a), AFM (1  $\mu\text{m} \times 1 \mu\text{m}$ ) (b) of the Col film, Col/Dp film, and Col/Dp-LA film

Dp and collagen, and the interaction resulted in a surface tightening of the film and an increase in surface roughness. These results were in agreement with the results of the SEM images.

### 3.2 Thermal and mechanical properties

Food packaging film with good thermal stability will effectively prevent the adverse effects of temperature on the performance of the film during summer transportation. The thermal stability of the Col film, Col/Dp film, and Col/Dp-LA film was determined by DSC. As can be seen in Fig. 2a, the denaturation temperature ( $T_d$ ) value of the Col film was 65.1  $^{\circ}\text{C}$ . An increase in  $T_d$  value of the film after the incorporation of Dp was obtained, and the  $T_d$  value of the Col/Dp film increased to 72.5  $^{\circ}\text{C}$ . The Col/Dp-LA film showed the highest thermal stability and the  $T_d$  value further increased to 75.5  $^{\circ}\text{C}$ . Similar increased trends in thermal stability were found in LA-catalyzed gallic acid crosslinked collagen hydrogels reported by Tang et al., and the  $T_d$  value from 67.4 to 74.7  $^{\circ}\text{C}$  [42]. The higher transition temperature suggested that LA effectively catalyzed the covalent crosslinking between Dp and collagen to enhance the thermal stability of the film.

Mechanical property is important for food packaging films because high mechanical strength can ensure the

integrity of food packaging in the process of transportation and reduce the risk of food spoilage caused by packaging damage [43]. The effects of Dp and LA on the mechanical strength including tensile strength (TS) and elongation at break (EAB) are shown in Fig. 2b, c. The Col/Dp-LA film showed the highest dry and wet TS of 134.05 MPa and 17.04 MPa compared to the Col film (92.31 MPa and 3.91 MPa) and Col/Dp film (121.44 MPa and 6.07 MPa). It was noticed that the EAB value of the film had a decreased trend after the use of LA. These results were attributed to the formation of multipoint Schiff base bounds between reactive o-quinones produced by LA catalyzed Dp and the amino groups of collagen chains. The strong covalent cross-linked bonds produced tighter connections between collagen and Dp, and this finding was consistent with the observations of the SEM and AFM images. The tighter connections hindered the movement of the collagen chains, resulting in a decrease in EAB. The dry and wet TS of the Col/Dp-LA film was superior to that of the transglutaminase-catalyzed gelatin-zein composite film (dry TS, 100.00 MPa) reported by Ahammed et al. [44], and that of the citric acid-crosslinked hemi-celluloses-based composite film (wet TS, 14.50 MPa) reported by Li et al. [45]. The results revealed that the

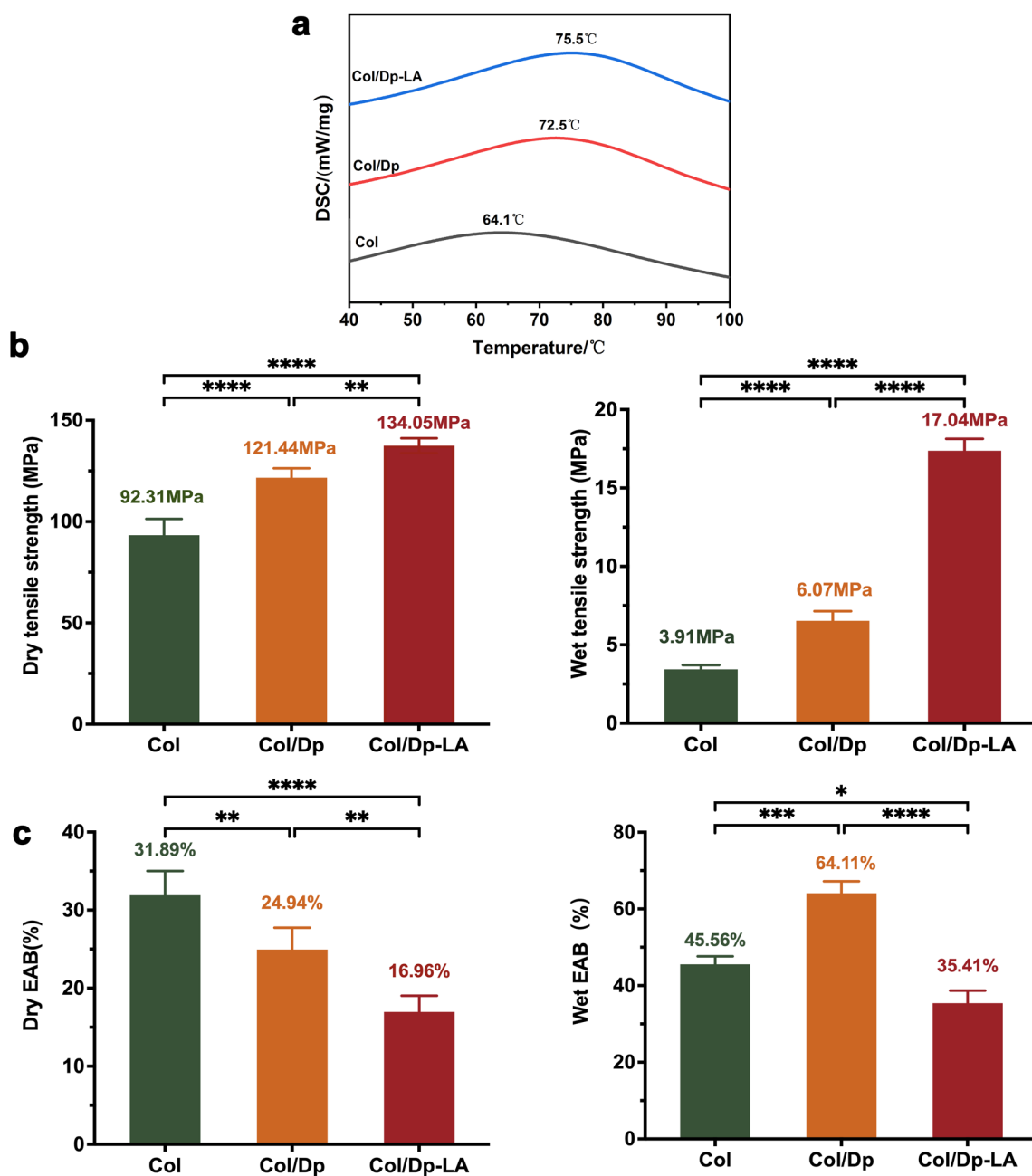


**Fig. 2** DSC curves (a), dry and wet tensile strength (b), and dry and wet elongation at break (c) of the Col film, Col/Dp film, and Col/Dp-LA film

use of the Col/Dp-LA film as food packaging film has more development potential than other natural-based films.

### 3.3 Barrier properties

#### 3.3.1 Water-resisting property

As a food packaging film, its good water-resisting property including low water vapor permeability (WVP) and water solubility are beneficial to prevent the growth of

microorganisms in packaged food. The water-resistant results of the Col film, Col/Dp film, and Col/Dp-LA film is summarized in Table 1. The WVP value of the Col film was  $1.77 \times 10^{-13} \text{ g}\cdot\text{mm}^{-1}\cdot\text{s}^{-1}\cdot\text{Pa}^{-1}$ , which decreased to  $1.30 \times 10^{-13} \text{ g}\cdot\text{mm}^{-1}\cdot\text{s}^{-1}\cdot\text{Pa}^{-1}$  after the addition of Dp into the collagen matrix. Compared with the Col film and the Col/Dp film, the Col/Dp-LA film had the lowest WVP value ( $1.04 \times 10^{-13} \text{ g}\cdot\text{mm}^{-1}\cdot\text{s}^{-1}\cdot\text{Pa}^{-1}$ ) ( $P < 0.05$ ). The catalysis of LA further decreased the WVP value of the



**Table 1** Thickness, water vapor permeability (WVP), and water solubility of the films

Film	Thickness (μm)	WVP (× 10 <sup>-13</sup> gmm <sup>-1</sup> s <sup>-1</sup> Pa <sup>-1</sup> )	Water solubility (%)
Col	28.4 ± 1.9	1.77 ± 0.12	11.22 ± 0.61
Dp/Col	32.4 ± 1.6 <sup>ns</sup>	1.30 ± 0.13 <sup>**</sup>	23.46 ± 2.31 <sup>****</sup>
Lac-Dp/Col	39.8 ± 1.8 <sup>**</sup>	1.04 ± 0.05 <sup>**</sup>	13.29 ± 1.79 <sup>ns</sup>

Values are presented as mean ± standard deviation (n = 3). All significance analyses were based on "Col". The number of asterisks in the same column indicates the significance of the difference, <sup>ns</sup>P > 0.05, <sup>\*\*</sup>P < 0.01, <sup>\*\*\*\*</sup>P < 0.0001

film, and this result was consistent with the findings of Luo et al. who detected that the WVP value of the film was reduced after adding LA to lignin-containing cellulose micro/nano-fibrils [46]. The compactness of the film increased with the formation of the covalent bonds between collagen and Dp catalyzed by LA, which further decreased the free volume of the film and restrained the diffusion rate of water vapor in the film [47]. In addition, the pyridine rings and aromatic in the Dp backbone played a filling role in the gap of the polymer matrix, and physically blocked the transfer of water vapor in the film [48].

The water solubility of the film presented a trend from rise to decline with the addition of Dp and LA in order, as shown in Table 1. This was because Dp contained plenty of hydrophilic hydroxyl groups that increased the hydrophilicity of the collagen film. With the LA catalysis, the phenolic hydroxyl groups of Dp were consumed so that the hydrophobicity of the film increased, and the water solubility decreased [49]. These results indicated that the use of LA improved the stability of the film under wet conditions, which was consistent with the wet strength results. The water solubility of the Col/Dp-LA film was 13.29%, which was lower than that of the chitosan/fish skin gelatin composite film (water solubility, 23.45%) reported by Li et al. [50] and the chitosan/

TEMPO-oxidized cellulose nanofibers film (water solubility, 51.6%) reported by Soni [51]. Therefore, the Col/Dp-LA film has better stability than other natural-based films under the wet state, which has wide application potential in developing water-resistant food packaging.

**3.3.2 Light barrier property**

The light barrier property of food packaging is very important to protect food quality and prolong food shelf life because light can trigger and accelerate the decomposition of nutrients in food and lead to food spoilage reactions [52]. The barrier effects of the film on UV and visible light are important indices to evaluate the light barrier property of the film. UV-barrier property of the film can protect the meat foods from oxidative deterioration, discoloration, and off-flavors [53]. The transmission spectrums of UV and visible light at the selected wavelength (200–800 nm) of all three films are shown in Fig. 3a. In the range of 200–400 nm, the Col/Dp-LA film blocked 80% of UV light transmission, while the Col film and the Col/Dp film blocked less than 40% of the UV light transmission. The increased UV-barrier property was caused by the UV absorption ability of the Schiff base bond between the quinone of LA-catalyzed Dp and the amino groups of collagen [35]. The Col/Dp-LA film exhibited excellent UV shielding property compared

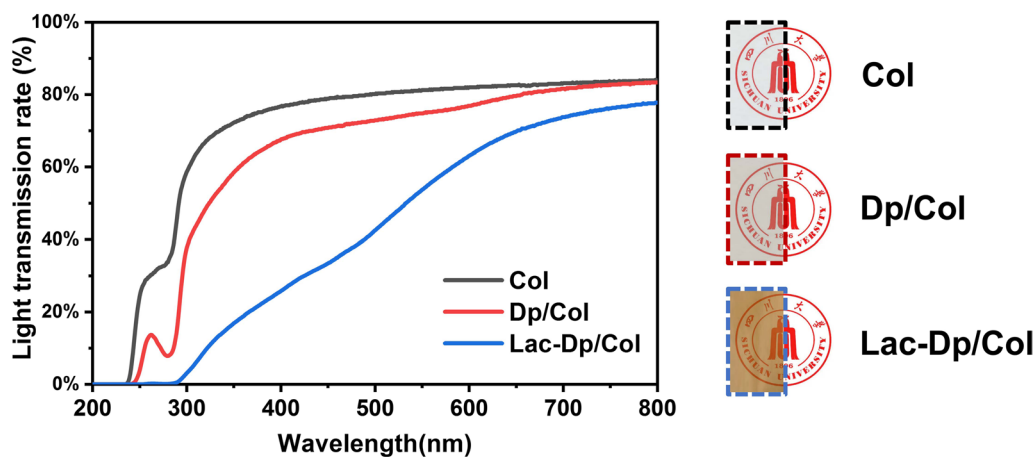


**Fig. 3** Light barrier property and the appearance comparison charts of the Col film, Col/Dp film, and Col/Dp-LA film

with the Col/Dp film and the Col film. In the visible light region, the light transmittance of the Col/Dp-LA film at 560 nm had an approximately 50% drop compared to the Col film, while the Col/Dp film only had a 10% drop. The performance enhancement could be explained by the studies of Wang et al. in which they found that the aromatic groups in phenolic compounds could absorb light [54]. Good light barrier property of the Col/Dp-LA film will have potential application in preventing the food quality change caused by ultraviolet light and visible light.

### 3.4 Antioxidant activity

Antioxidant food packaging can inhibit the oxidative decomposition of food by releasing antioxidants to prevent the production of harmful substances and prolong the shelf life of food. The free radicals scavenging rates of DPPH and ABTS are commonly used to characterize the antioxidant activity of food packaging. As shown in Fig. 4, the Col film exhibited poor antioxidant activity and merely scavenged 12.07% ABTS free radicals and 7.23% DPPH free radicals. The Col/Dp-LA film scavenged 65.10% ABTS free radicals and 66.04% DPPH free radicals, which showed a slight reduction of antioxidation activity in comparison to the Col/Dp film. Even though, the antioxidant activity of the Col/Dp-LA film was still higher than that of the chitosan/tea polyphenol composite film (DPPH, 40%) reported by Chen et al. [49]. The antioxidant activity increased in the order of Col/Dp film > Col/Dp-LA film > Col film. This was because the addition of Dp conferred good antioxidant activity on the collagen film, while the catalyzing of LA caused the phenolic hydroxyl group of Dp to be oxidized to quinone, resulting in a decrease in the number of phenolic

hydroxyl groups and thus a decrease in the antioxidant activity of the Col/Dp-LA film.

### 3.5 Color variation of the Col/Dp-LA/VOP film in different pH solutions

In order to verify that VOP still has pH sensitivity after loading VOP onto the Col/Dp-LA film, the color change trends of VOP solution and the Col/Dp-LA/VOP film under different pH conditions were compared, and the results are shown in Fig. 5. With the sequential increase of pH, the color of VOP solution changed from purple-red to blue-purple, and the maximum absorption peak of the solution shifted from 517 to 570 nm (Fig. 5a). The Col/Dp-LA/VOP film showed a color change consistent with that of VOP solution at different pH conditions, as shown in Fig. 5b. These changes might be due to the different structures of VOP at different pH conditions. A similar finding was found by Wu et al. who tested the color and UV spectra changes of black rice anthocyanins under different pH conditions [55]. In the acidic medium, the flavylium cation dominated, and VOP solution showed a red color at this time. With the pH increased, VOP lost the cation on epoxide C and was simultaneously attacked by nucleophilic groups in water, resulting in a hydration reaction that formed colorless pseudo-base methanol. In alkaline solutions, the flavylium cation lost its proton, and the blue/purple intensity of the quinone base increased with increasing pH, then the solution was blue-purple [56]. In addition, the thermal stability, mechanical properties, water resistance, light transmission, and antioxidant activity of the Col/Dp-LA/VOP film were tested. The results showed that the addition of VOP has no negative effect on the physicochemical properties of the film. Detailed

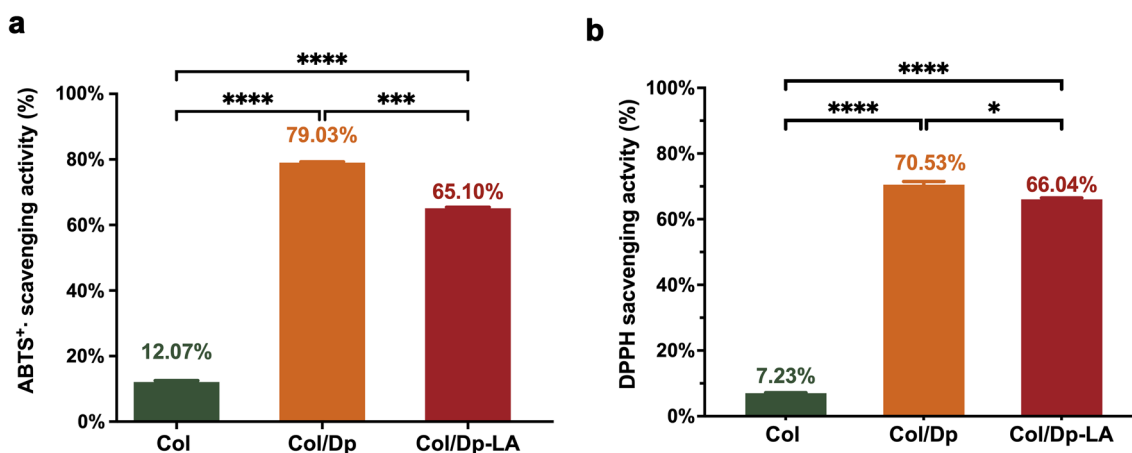
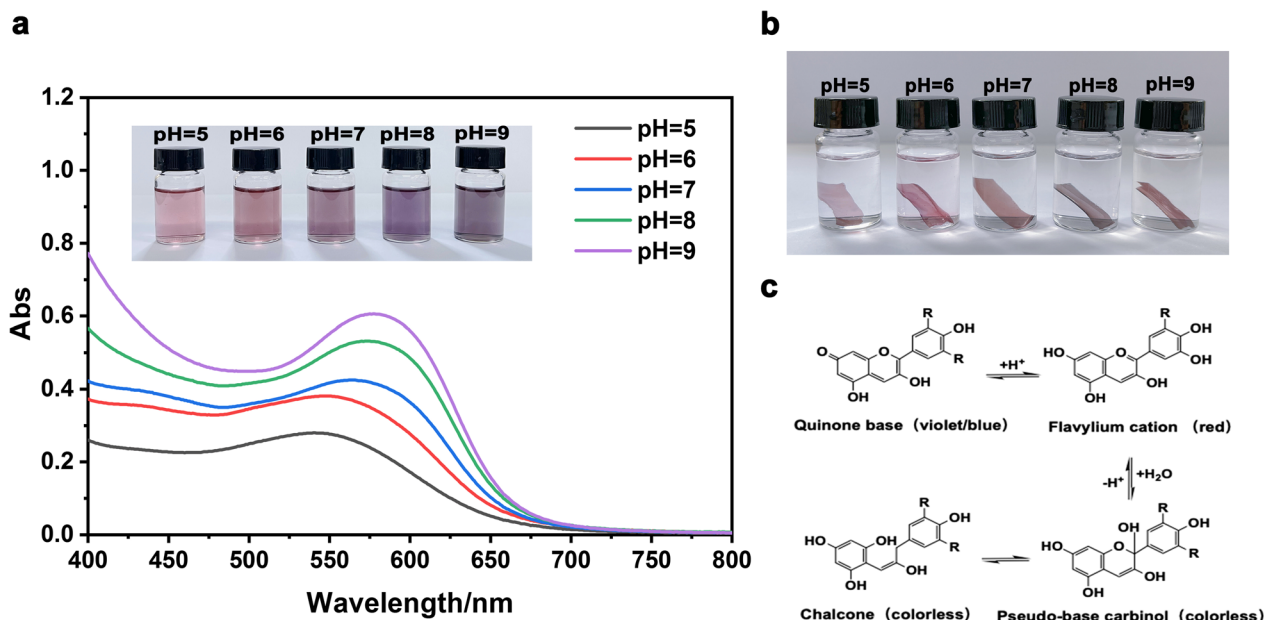


Fig. 4 ABTS (a), DPPH (b) free radical scavenging rates of the Col film, Col/Dp film, and Col/Dp-LA film



**Fig. 5** UV-Vis spectra of VOP solutions (a), the color changes of the Col/Dp-LA/VOP film immersed in different pH solutions (pH 5.0–9.0) (b), and the structural transformation of VOP in the acid–base conditions (c)

data were provided in the Additional file 1: Fig. S3–S5 and Table S1.

### 3.6 Application of the Col/Dp-LA/VOP film for monitoring the freshness of fish

Lipid oxidation produces alkanes, aldehydes, and volatile basic nitrogenous compounds that are responsible for meat rancidity, and the contents of these substances can cause changes in the pH value of meat and can be reflected by TBARs, TVB-N, and pH values. The TBARs, TVB-N, and pH value of the fish fillets packaged in the Col film and the Col/Dp-LA/VOP film during 10 d at 4 °C are displayed in Fig. 6. As can be seen in Fig. 6a, the TBARs value of the fillets packaged in the Col/Dp-LA/VOP film was significantly lower than that in the Col film. On the sixth day, the color of the fish fillets packaged in the Col film exhibited obvious oxidative reddening, while those in the Col/Dp-LA/VOP film had no obvious color change. This observation could be explained by the better antioxidant activity and light barrier property of the Col/Dp-LA film.

TVB-N value is a commonly used parameter to characterize the freshness of meat. As shown in Fig. 6b, the rate of increase in the TVB-N value of meat packaged in the Col film was much higher than that in the Col/Dp-LA/VOP film. The TVB-N value of the fish fillets packaged in the Col film was increased to 16.9 mg/100 g on the 6th day, which obviously exceeded Chinese rejection standard limits of 15 mg/100 g, showing that the fillets packaged in the Col film were rotten at the 6<sup>th</sup> day. At the

same time, the TVB-N value of the fish fillets packaged in the Col/Dp-LA/VOP film was 13.8 mg/100 g at 6th day, and it reached 17.1 mg/100 g at 8th day along with the color of the film changed from purplish-red to grayish-blue. This result demonstrated that the Col/Dp-LA/VOP film could prolong the shelf life of the fish 2 days. The results of TVB-N were in agreement with the results of TBARs.

As can be seen from Fig. 6c, the pH value of the fish had a trend of decreasing and then increasing during the fish storage. The decrease in pH was caused by the lactic acid from anaerobic glycogen deterioration in fish and the phosphoric acid from triphosphate adenosine degradation in fish. With the extension of storage, protein degradation and bacterial proliferation of the fish produced alkaline autolysis compounds which elevated pH value [57]. The color of the Col/Dp-LA/VOP film changed significantly from purplish-red to greyish-blue with the changes in pH value caused by fish spoilage. The Col/Dp-LA/VOP film could be further explored the application as active/intelligent food packaging by prolonging the shelf life of food and providing a simple visual color change to monitor the freshness of packaged protein- and fat-rich food.

## 4 Conclusions

In this work, we designed a collagen-based active and intelligent packaging film with high strength by treating with Dp and LA and incorporating with VOP. The effects of Dp and LA on the structure and properties of

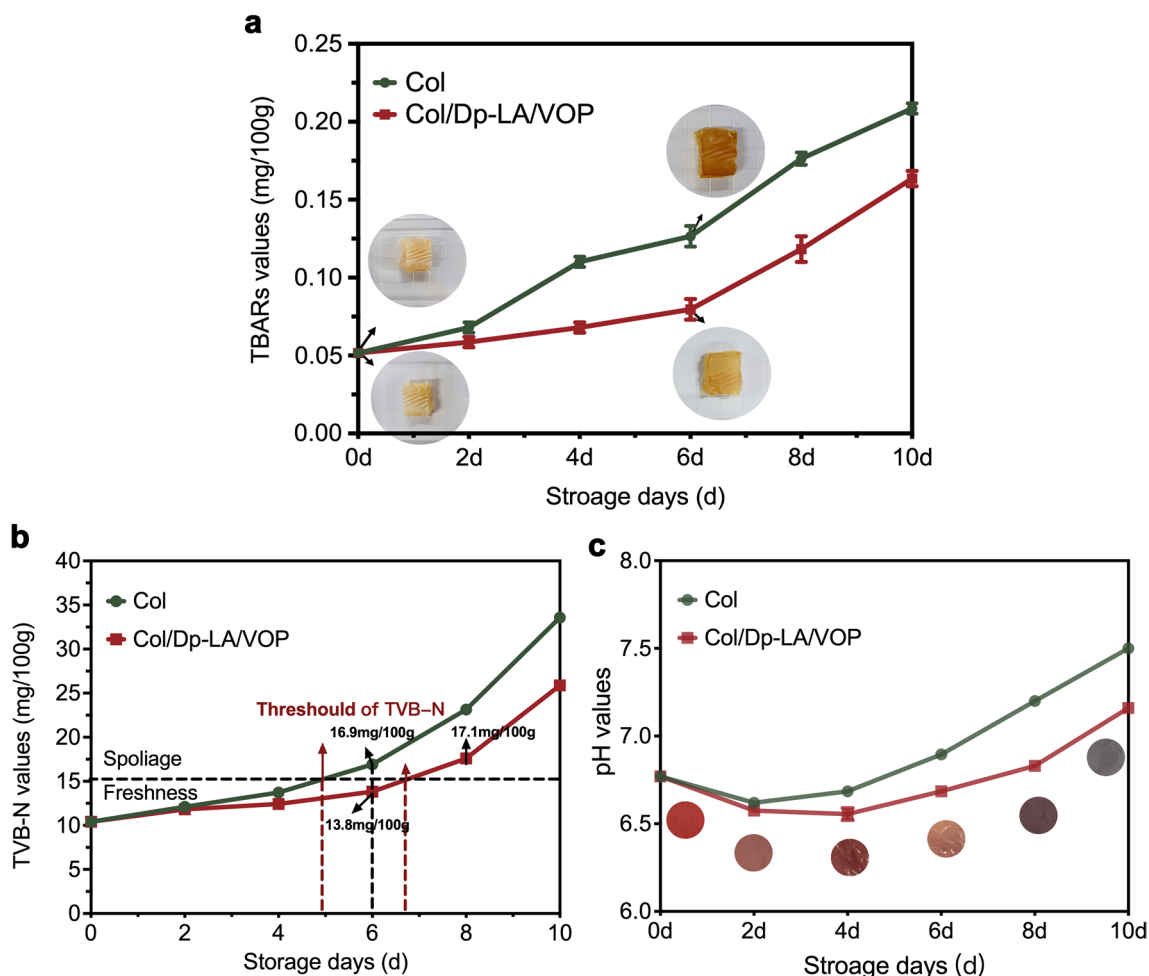


**Fig. 6** The TBARs values and photograph (a), TVB-N values (b), pH values (c) of the fish fillets wrapped in the Col film and Col/Dp-LA/VOP film, respectively, and the color changes of the Col/Dp-LA/VOP film for monitoring the fish freshness at 4 °C for 10 days (c)

collagen film were discussed. The results of SEM and AFM images showed the addition of LA brought tighter connections between Dp and collagen. The collagen film treated with Dp and LA exhibited excellent mechanical strength, thermal stability, water-resisting property, light barrier property, and antioxidant activity. Moreover, the addition of VOP introduced the pH-sensitivity property into the film, and the Col/Dp-LA/VOP film exhibited a continuous color change with increasing pH from 5.0 to 9.0. The potential application of the Col/Dp-LA/VOP film as an intelligent packaging film was evaluated by packaging the fish fillets to monitor the freshness of the fish. The film showed a remarkable color response from purplish-red to grayish-blue with the spoilage of fish stored at 4 °C for 10 days. From the TVB-N and TBARs values, the Col/Dp-LA/VOP film effectively prolonged the shelf life and inhibited lipid peroxidation of the fish fillets. In the future, the Col/Dp-LA/VOP film might be a potential candidate in the active and intelligent food

packaging industry, especially for protein- and lipid-rich food, such as casings in the meat industry.

**Abbreviations**

Dp	Delphinidin
LA	Laccase
Dp-LA	Laccase-catalyzed delphinidin
FT-IR	Fourier transform infrared spectrometer
SEM	Scanning electron microscope
AFM	Atomic force microscope
TS	Tensile strength
EAB	Elongation at break
DSC	Differential scanning calorimetry
WVP	Water vapor permeability
ABTS	2,2'-Azinobis-(3-ethylbenzthiazoline-6-sulphonate)
DPPH	1,1-Diphenyl-2-picrylhydrazyl radical
VOP	<i>Vaccinium oxycoccus</i> Pigment
TBARs	Thiobarbituric acid reactive substances
TVB-N	Total volatile basic nitrogen
T <sub>d</sub>	Denaturation temperature
H	Hours
D	Days
Min	Minutes

## Supplementary Information

The online version contains supplementary material available at <https://doi.org/10.1186/s42825-023-00118-6>.

**Additional file 1: Fig. S1.** FT-IR spectra of the Col film, Col/Dp film, and Col/Dp-LA film. **Fig. S2.** High-resolution C1s XPS spectra of the Col film, Col/Dp film, and Col/Dp-LA film. **Fig. S3.** DSC(a), dry and wet tensile strength (b), dry and wet elongation at break. (c) **Fig. S4.** Light barrier property of the Col/Dp-LA film and the Col/Dp-LA/VOP film. **Fig. S5.** ABTS(a), DPPH(b) free radical scavenging rates of the Col/Dp-LA film and the Col/Dp-LA/VOP film. **Table S1.** Thickness, Water vapor permeability (WVP), and water solubility of the Col/Dp-LA film and Col/Dp-LA/VOP film.

### Author contributions

SMY: conceptualization, methodology, writing-original draft, writing-review & editing. YZZ: reviewing, investigation, visualization, editing of the manuscript. XXZ: data curation, visualization. KYT: reviewing. GYL: supervision, project administration, funding acquisition, writing, reviewing, and editing of the manuscript. All authors read and approved the final manuscript.

### Funding

This study was supported by the National Natural Science Foundation of China (No. 22078206).

### Availability of data and materials

The datasets used and analyzed during the current study are available from the corresponding author on reasonable request.

### Declaration

#### Competing interests

The authors of this manuscript have no conflicts of interest to disclose.

#### Author details

<sup>1</sup>College of Biomass Science and Engineering, Key Laboratory of Leather Chemistry and Engineering of Ministry of Education, Sichuan University, Chengdu 610065, China. <sup>2</sup>School of Chemical Engineering, The University of Queensland, Brisbane, QLD 4072, Australia.

Received: 7 February 2023 Revised: 2 April 2023 Accepted: 3 April 2023

Published online: 13 April 2023

### References

- Zhang WL, Rhim JW. Recent progress in konjac glucomannan-based active food packaging films and property enhancement strategies. *Food Hydrocolloids*. 2022. <https://doi.org/10.1016/j.foodhyd.2022.107572>.
- Wang WH, Liu YW, Liu AJ, Zhao YN, Chen X. Effect of in situ apatite on performance of collagen fiber film for food packaging applications. *J Appl Polym Sci*. 2016. <https://doi.org/10.1002/app.44154>.
- Yu ZL, Dhital R, Wang W, Sun L, Zeng WC, Mustapha A, Lin MS. Development of multifunctional nanocomposites containing cellulose nanofibrils and soy proteins as food packaging materials. *Food Packag Shelf Life*. 2019. <https://doi.org/10.1016/j.fpsl.2019.100366>.
- Dong MX, Tian LJ, Li JY, Jia J, Dong YF, Tu YG, Liu XB, Tan C, Duan X. Improving physicochemical properties of edible wheat gluten protein films with proteins, polysaccharides and organic acid. *Lwt Food Sci Technol*. 2022. <https://doi.org/10.1016/j.lwt.2021.112868>.
- Bhawani SA, Hussain H, Bojo O, Fong SS. Proteins as agricultural polymers for packaging production. In: *Bionanocomposites for packaging applications*. 2018;13:243–67. [https://doi.org/10.1007/978-3-319-67319-6\\_13](https://doi.org/10.1007/978-3-319-67319-6_13)
- Irastorza A, Zaranonda I, Andonegi M, Guerrero P, de la Caba K. The versatility of collagen and chitosan: from food to biomedical applications. *Food Hydrocolloids*. 2021. <https://doi.org/10.1016/j.foodhyd.2021.106633>.
- Mir SA, Dar BN, Wani AA, Shah MA. Effect of plant extracts on the techno-functional properties of biodegradable packaging films. *Trends Food Sci Technol*. 2018;80:141–54.
- Lorenzo JM, Battlle R, Gomez M. Extension of the shelf-life of foal meat with two antioxidant active packaging systems. *Lwt Food Sci Technol*. 2014;59(1):181–8. <https://doi.org/10.1016/j.lwt.2014.04.061>.
- Zhang Y, Wang BY, Lu FF, Wang L, Ding YH, Kang XY. Plant-derived antioxidants incorporated into active packaging intended for vegetables and fatty animal products: a review. *Food Addit Contam Part A Chem Anal Control Expo Risk Assess*. 2021;38(7):1237–48. <https://doi.org/10.1080/19440049.2021.1885745>.
- Roy S, Rhim JW. Carrageenan/agar-based functional film integrated with zinc sulfide nanoparticles and Pickering emulsion of tea tree essential oil for active packaging applications. *Int J Biol Macromol*. 2021;193:2038–46. <https://doi.org/10.1016/j.jbiomac.2021.11.035>.
- Qu WJ, Xiong T, Wang B, Li YH, Zhang XX. The modification of pomegranate polyphenol with ultrasound improves mechanical, antioxidant, and antibacterial properties of tuna skin collagen-chitosan film. *Ultrason Sonochem*. 2022. <https://doi.org/10.1016/j.ultsonch.2022.105992>.
- An XS, Duan SJ, Jiang ZC, Chen WX, Sun WX, Liu XY, Sun ZH, Li YP, Yan MY. Role of chlorogenic acid and procyanidin in the modification of self-assembled fibrillar gel prepared from tilapia collagen. *Polym Degrad Stab*. 2022. <https://doi.org/10.1016/j.polymdegradstab.2022.110177>.
- Yu ZL, Sun L, Wang W, Zeng WC, Mustapha A, Lin MS. Soy protein-based films incorporated with cellulose nanocrystals and pine needle extract for active packaging. *Ind Crops Prod*. 2018;112:412–9. <https://doi.org/10.1016/j.indcrop.2017.12.031>.
- Liu K, Chen SG, Chen HB, Tong P, Gao JY. Cross-linked ovalbumin catalyzed by polyphenol oxidase: preparation, structure and potential allergenicity. *Int J Biol Macromol*. 2018;107:2057–64. <https://doi.org/10.1016/j.jbiomac.2017.10.072>.
- Benbettaieb N, Gay JP, Karbowski T, Debeaufort F. Tuning the functional properties of polysaccharide-protein bio-based edible films by chemical, enzymatic, and physical cross-linking. *Compr Rev Food Sci Food Saf*. 2016;15(4):739–52. <https://doi.org/10.1111/1541-4337.12210>.
- Bulusu G, Desiraju GR. Strong and weak hydrogen bonds in protein-ligand recognition. *J Indian Inst Sci*. 2020;100(1):31–41. <https://doi.org/10.1007/s41745-019-00141-9>.
- Mayolo-Deloisa K, Gonzalez-Gonzalez M, Rito-Palomares M. Laccases in food industry: bioprocessing, potential industrial and biotechnological applications. *Front Bioeng Biotechnol*. 2020. <https://doi.org/10.3389/fbioe.2020.00222>.
- Mattinen ML, Hellman M, Permi P, Autio K, Kalkkinen N, Buchert J. Effect of protein structure on laccase-catalyzed protein oligomerization. *J Agric Food Chem*. 2006;54(23):8883–90. <https://doi.org/10.1021/jf062397h>.
- Nady N, Schroen K, Franssen MCR, van Lagen B, Murali S, Boom RM, Mohyeldin MS, Zuillhof H. Mild and highly flexible enzyme-catalyzed modification of poly(ethersulfone) membranes. *ACS Appl Mater Interfaces*. 2011;3(3):801–10. <https://doi.org/10.1021/am101155e>.
- Bozic M, Gorgieva S, Kokol V. Laccase-mediated functionalization of chitosan by caffeic and gallic acids for modulating antioxidant and antimicrobial properties. *Carbohydr Polym*. 2012;87(4):2388–98. <https://doi.org/10.1016/j.carbpol.2011.11.006>.
- Jus S, Stachel I, Schloegl W, Pretzler M, Friess W, Meyer M, Birner-Gruenberger R, Guebitz GM. Cross-linking of collagen with laccases and tyrosinases. *Mater Sci Eng C Mater Biol Appl*. 2011;31(5):1068–77. <https://doi.org/10.1016/j.msec.2011.03.007>.
- Tian X, Wang Y, Duan S, Hao Y, Zhao K, Li Y, Dai R, Wang W. Evaluation of a novel nano-size collagenous matrix film cross-linked with gallotannins catalyzed by laccase. *Food Chem*. 2021;351:129335. <https://doi.org/10.1016/j.foodchem.2021.129335>.
- Neves D, Andrade PB, Videira RA, de Freitas V, Cruz L. Berry anthocyanin-based films in smart food packaging: a mini-review. *Food Hydrocolloids*. 2022. <https://doi.org/10.1016/j.foodhyd.2022.107885>.
- Hu HX, Yao XY, Qin Y, Yong HM, Liu J. Development of multifunctional food packaging by incorporating betalains from vegetable amaranth (*Amaranthus tricolor* L.) into quaternary ammonium chitosan/fish gelatin blend films. *Int J Biol Macromol*. 2020;159:675–84. <https://doi.org/10.1016/j.jbiomac.2020.05.103>.
- Etxabide A, Kilmartin PA, Mate JL. Color stability and pH-indicator ability of curcumin, anthocyanin and betanin containing colorants under different storage conditions for intelligent packaging development. *Food Control*. 2021. <https://doi.org/10.1016/j.foodcont.2020.107645>.

26. Kong J, Ge X, Sun Y, Mao M, Yu H, Chu R, Wang Y. Multi-functional pH-sensitive active and intelligent packaging based on highly cross-linked zein for the monitoring of pork freshness. *Food Chem.* 2022;404(Pt B):134754. <https://doi.org/10.1016/j.foodchem.2022.134754>.
27. Moghadam M, Salami M, Mohammadian M, Emam-Djomeh Z. Development and characterization of pH-sensitive and antioxidant edible films based on mung bean protein enriched with *Echium amoenum* anthocyanins. *J Food Meas Charact.* 2021;15(4):2984–94. <https://doi.org/10.1007/s11694-021-00872-3>.
28. Shi C, Zhang J, Jia Z, Yang X, Zhou Z. Intelligent pH indicator films containing anthocyanins extracted from blueberry peel for monitoring tilapia fillet freshness. *J Sci Food Agric.* 2021;101(5):1800–11. <https://doi.org/10.1002/jsfa.10794>.
29. Ran RM, Chen SY, Su YH, Wang LY, He SJ, He BB, Li C, Wang CX, Liu YT. Preparation of pH-colorimetric films based on soy protein isolate/ZnO nanoparticles and grape-skin red for monitoring pork freshness. *Food Control.* 2022. <https://doi.org/10.1016/j.foodcont.2022.108958>.
30. Yong H, Liu J, Kan J, Liu J. Active/intelligent packaging films developed by immobilizing anthocyanins from purple sweetpotato and purple cabbage in locust bean gum, chitosan and kappa-carrageenan-based matrices. *Int J Biol Macromol.* 2022;211:238–48. <https://doi.org/10.1016/j.ijbiomac.2022.05.046>.
31. Yang H, Li Q, Liu S, Li G. Acetic acid/1-ethyl-3-methylimidazolium acetate as a biphasic solvent system for altering the aggregation behavior of collagen molecules. *J Mol Liq.* 2018;262:78–85.
32. Chen J, Luo LC, Cen CN, Liu YA, Li H, Wang YB. The nano antibacterial composite film carboxymethyl chitosan/gelatin/ nano ZnO improves the mechanical strength of food packaging. *Int J Biol Macromol.* 2022;220:462–71. <https://doi.org/10.1016/j.ijbiomac.2022.08.005>.
33. Liu J, Wang H, Wang P, Guo M, Jiang S, Li X, Jiang S. Films based on κ-carrageenan incorporated with curcumin for freshness monitoring. *Food Hydrocolloids.* 2018;83(OCT):134–42.
34. Choo KW, Lin M, Mustapha A. Chitosan/acylated starch composite films incorporated with essential oils: physicochemical and antimicrobial properties. *Food Biosci.* 2021;43:101287. <https://doi.org/10.1016/j.foodb.2021.101287>.
35. Tang P, Zheng T, Yang C, Li G. Enhanced physicochemical and functional properties of collagen films cross-linked with laccase oxidized phenolic acids for active edible food packaging. *Food Chem.* 2022;393:133353. <https://doi.org/10.1016/j.foodchem.2022.133353>.
36. Cao YM, Gu WG, Zhang JJ, Chu Y, Ye XQ, Hu YQ, Chen JC. Effects of chitosan, aqueous extract of ginger, onion and garlic on quality and shelf life of stewed-pork during refrigerated storage. *Food Chem.* 2013;141(3):1655–60. <https://doi.org/10.1016/j.foodchem.2013.04.084>.
37. Apriyani RN, Arpah S, AOAC. Official methods of analysis of the Association of Official Analytical Chemists. Washington: AOAC; 1995.
38. Qiang TT, Chen L, Yan Z, Liu XH. Evaluation of a novel collagenous matrix membrane cross-linked with catechins catalyzed by laccase: a sustainable biomass. *J Agric Food Chem.* 2019;67(5):1504–12. <https://doi.org/10.1021/acs.jafc.8b05810>.
39. Milczek EM. Commercial applications for enzyme-mediated protein conjugation: new developments in enzymatic processes to deliver functionalized proteins on the commercial scale. *Chem Rev.* 2018;118(1):119–41. <https://doi.org/10.1021/acs.chemrev.6b00832>.
40. Adamiak K, Sionkowska A. The influence of UV irradiation on fish skin collagen films in the presence of xanthohumol and propanediol. *Spectrochim Acta A Mol Biomol Spectrosc.* 2022;282:121652. <https://doi.org/10.1016/j.saa.2022.121652>.
41. Wu C, Li Y, Du Y, Wang L, Tong C, Hu Y, Pang J, Yan Z. Preparation and characterization of konjac glucomannan-based bionanocomposite film for active food packaging. *Food Hydrocolloids.* 2019;89(APR):682–90.
42. Tang P, Zheng T, Shen L, Li G. Properties of bovine type I collagen hydrogels cross-linked with laccase-catalyzed gallic acid. *Polym Degrad Stab.* 2021;189(3):109614.
43. Cazon P, Vazquez M. Mechanical and barrier properties of chitosan combined with other components as food packaging film. *Environ Chem Lett.* 2020;18(2):257–67. <https://doi.org/10.1007/s10311-019-00936-3>.
44. Ahammed S, Liu F, Wu JM, Khin MN, Yokoyama WH, Zhong F. Effect of transglutaminase crosslinking on solubility property and mechanical strength of gelatin-zein composite films. *Food Hydrocolloids.* 2021. <https://doi.org/10.1016/j.foodhyd.2021.106649>.
45. Li JY, Liu YX, Sun B, Zhang RF. Improving the wet strength of hemicelluloses based composite films by citric acid crosslinking. *J Wood Chem Technol.* 2020;41(1):1–9. <https://doi.org/10.1080/02773813.2020.1847147>.
46. Luo JQ, Su YQ, Chen JH, Wang XH, Liu JG. Pretreatment of lignin-containing cellulose micro/nano-fibrils (LCMNF) from corn cob residues. *Cellulose.* 2021;28(8):4671–84. <https://doi.org/10.1007/s10570-021-03798-7>.
47. Hu XX, Liu YF, Zhu DD, Jin YG, Jin HB, Sheng L. Preparation and characterization of edible carboxymethyl cellulose films containing natural antibacterial agents: lysozyme. *Food Chem.* 2022. <https://doi.org/10.1016/j.foodchem.2022.132708>.
48. Zhuang YL, Ruan SY, Yao HH, Sun Y. Physical properties of composite films from tilapia skin collagen with Pachyrhizus starch and rambutan peel phenolics. *Mar Drugs.* 2019. <https://doi.org/10.3390/md17120662>.
49. Chen T, Shen YF, Wu D, Wu R, Sheng J, Feng X, Tang XZ. Biodegradable films of chitosan and tea polyphenols catalyzed by laccase and their physical and antioxidant activities. *Food Biosci.* 2022. <https://doi.org/10.1016/j.foodb.2021.101513>.
50. Li YJ, Tang CM, He QF. Effect of orange (*Citrus sinensis* L.) peel essential oil on characteristics of blend films based on chitosan and fish skin gelatin. *Food Biosci.* 2021. <https://doi.org/10.1016/j.foodb.2021.100927>.
51. Soni B, Hassan E, Schilling MW, Mahmoud B. Transparent bionanocomposite films based on chitosan and TEMPO-oxidized cellulose nanofibers with enhanced mechanical and barrier properties. *Carbohydr Polym.* 2016;151:779–89. <https://doi.org/10.1016/j.carbpol.2016.06.022>.
52. Cazon P, Vazquez M, Velazquez G. Cellulose-glycerol-polyvinyl alcohol composite films for food packaging: evaluation of water adsorption, mechanical properties, light-barrier properties and transparency. *Carbohydr Polym.* 2018;195:432–43. <https://doi.org/10.1016/j.carbpol.2018.04.120>.
53. Ma Q, Du L, Yang Y, Wang L. Rheology of film-forming solutions and physical properties of tara gum film reinforced with polyvinyl alcohol (PVA). *Food Hydrocolloids.* 2017;63(Feb):677–84.
54. Wang XC, Yong HM, Gao L, Li LL, Jin MJ, Liu J. Preparation and characterization of antioxidant and pH-sensitive films based on chitosan and black soybean seed coat extract. *Food Hydrocolloids.* 2019;89:56–66. <https://doi.org/10.1016/j.foodhyd.2018.10.019>.
55. Wu C, Sun J, Zheng P, Kang X, Chen M, Li Y, Ge Y, Hu Y, Pang J. Preparation of an intelligent film based on chitosan/oxidized chitin nanocrystals incorporating black rice bran anthocyanins for seafood spoilage monitoring. *Carbohydr Polym.* 2019;222:115006. <https://doi.org/10.1016/j.carbpol.2019.115006>.
56. de Oliveira JG, Braga ARC, de Oliveira BR, Gomes FP, Moreira VL, Pereira VAC, Egea MB. The potential of anthocyanins in smart, active, and bioactive eco-friendly polymer-based films: a review. *Food Res Int.* 2021. <https://doi.org/10.1016/j.foodres.2021.110202>.
57. Kim HH, Ryu SH, Jeong SM, Kang WS, Lee JE, Kim SR, Xu X, Lee GH, Ahn DH. Effect of high hydrostatic pressure treatment on urease activity and inhibition of fishy smell in mackerel (*Scomber japonicus*) during storage. *J Microbiol Biotechnol.* 2021;31(12):1684–91. <https://doi.org/10.4014/jmb.2106.06052>.

## Publisher's Note

Springer Nature remains neutral with regard to jurisdictional claims in published maps and institutional affiliations.